

## 2D and 3D Modelling Electrical Resistivity Tomography (ERT) of Landslide Sliding and Weak Bedding Plane Along Mountain Road North Bengkulu-Lebong, Indonesia

Suhendra<sup>1,2\*</sup>, Jesika Erni Elfrita Sinaga<sup>1,2</sup>, Darmawan Ikhlas Fadli<sup>1,2,3</sup>, Halauddin<sup>1,2</sup>, Supiyati<sup>4</sup>

<sup>1</sup>Department of Geophysics, Faculty of Mathematics and Natural Sciences, University of Bengkulu, Bengkulu, 38122, Indonesia

<sup>2</sup>Shallow Groundwater and Mineral Exploration Research Group, Department of Geophysics, Faculty of Mathematics and Natural Sciences, University of Bengkulu, Bengkulu, 38122, Indonesia

<sup>3</sup>Center for Disaster Mitigation Studies, Research Institutions and Community Service. University of Bengkulu, Bengkulu, 38122, Indonesia

<sup>4</sup>Department of Physics, Faculty of Mathematics and Natural Sciences, University of Bengkulu, Bengkulu, 38122, Indonesia

\*Corresponding author, email : [suhendra@unib.ac.id](mailto:suhendra@unib.ac.id)

### ARTICLE INFO

Received :  
14 February 2023

Revised :  
12 March 2024

Accepted :  
29 March 2024

Published :  
7 April 2024

### ABSTRACT

The North Bengkulu-Lebong Mountain Road is prone to landslide disasters due to its geological susceptibility to land movement. This study aims to measure and assess the sliding plane on the mountain road, particularly in the layer with a soft rock structure, such as clay rock. The study utilizes 2D and 3D Electrical Resistivity Tomography (ERT) methods with the Wenner-Schlumberger configuration to measure the resistivity of the rock layers. The research includes one 2D measurement point and one 3D ERT measurement point, estimating actual resistivity values in each rock layer. Our results identify triggering and controlling factors for landslide disasters in the research area. The geological conditions consist of layers of clay (200-500  $\Omega\text{m}$ ), wet clay (500-900  $\Omega\text{m}$ ), dry clay (1000-3000  $\Omega\text{m}$ ), weathering clay (500-1000  $\Omega\text{m}$ ), aquifer (10-65  $\Omega\text{m}$ ), perched aquifer (100-200  $\Omega\text{m}$ ), weathering igneous rock (>10000  $\Omega\text{m}$ ), and massive intrusive rock (>20000  $\Omega\text{m}$ ). These geological conditions significantly influence the strength of landslide materials, with the sliding of the soft rock layer causing landslides and resulting in a large volume of landslide material. Other contributing factors to landslides in this location include slope, topography, and hydrology, with extreme slopes ranging from 33° to 55°, making it a very steep area with high potential for landslides.

**Keywords** : 2D ERT; 3D ERT; Landslide Sliding; Weak Bedding; Mountain Road

### INTRODUCTION

Bengkulu is a province in Indonesia with a pronounced risk of landslides, particularly evident along the North Bengkulu-Lebong Mountain Road, situated in a mountainous region (BPBD, 2019). This area is highly susceptible to land movement disasters, as highlighted by Ouimet et al. (2007). The geological characteristics of the North Bengkulu-Lebong Mountain Road, located within the Sumatran fault zone, extend from south to north, resulting in steep slopes (Ariyanto & Joni, 2019). Functioning as a crucial transportation route connecting Lebong Regency with other regions in Bengkulu Province, the North Bengkulu-Lebong Mountain Road is in close proximity to residential areas and has isolated several sub-districts. The morphology and topography of this cross-district mountain road are hilly and sloping, characterized by high

steepness, posing a significant risk to road users in the event of landslides (Smethurst et al., 2017). Bengkulu Province, including the study area, experiences relatively high annual rainfall, averaging between 235-280 mm/year (BMKG, 2012). These environmental conditions collectively render the North Bengkulu-Lebong Mountain Road highly susceptible to land movement, commonly known as landslides.

Various factors contribute to the occurrence of ground motion, including rainfall (Wieczorek & Jäger, 1996), rock structure (Agliardi et al., 2013), slope, and land use (Hugenschmidt, 2010; Smethurst et al., 2017), as well as earthquakes (Huang & Fan, 2013). The North Bengkulu-Lebong Mountain Road serves as a highly active and busy transportation route for land transportation. Vibrations generated by the constant movement of vehicles on this route can induce ground motion, leading to changes in the physical properties of the soil on the surface (Ismail et al., 2002; Maslin, 2015). These land movement disasters can have severe impacts if not handled properly, leading to economic problems (Dai et al., 2002). An illustrative example is the landslide event in 2021. The community experienced the disruptive effects of the landslide disaster in 2021, notably the disruption of the land transportation system on this route as the road was entirely covered by landslide material.

Landslides have a significant impact on road users, emphasizing the importance of taking initial steps to minimize potential effects, commonly known as landslide mitigation and management (Dai et al., 2002). One mitigation strategy to reduce the risk of landslides involves understanding the rock structure to prevent or control ground motion (Soeters & Westen, 1996). To identify and mark areas prone to ground motion, it is essential to conduct detailed and thorough measurements of the rock layer, including lithology, depth, structure, and landslide sliding in locations that have experienced ground motion. The 2D and 3D Electrical Resistivity Tomography (ERT) method is employed for this purpose (Boyd et al., 2021; Grifka et al., 2022).

The study and investigation of landslide slidings can be conducted using various geophysical methods (Jongmans & Garambois, 2007), one of which is the resistivity geoelectric method. This method is widely utilized for assessing external surfaces with the potential for landslides (Shevnin et al., 2007). A case study of landslide sliding was carried out using the geoelectric resistivity method in Kebarongan Village, Kemranjen Subdistrict, Banyumas Regency. The interpretation results revealed that the lithology of Kebarongan village comprises four soil layers. The topsoil consists of sandy clay, wet clay, and sandy clay (Sugito & Jati, 2010). The 2D and 3D Electrical Resistivity Tomography (ERT) method is frequently employed in landslide case studies to examine the rock structure, bedrock, and landslide sliding (Bell et al., 2006; Grifka et al., 2022; Hojat et al., 2019; Lapenna et al., 2003; Souisa et al., 2018; Supper et al., 2014).

The condition of each landslide sliding found at each location exhibits unique characteristics, making it challenging to generalize solutions for other places. Appropriate landslide mitigation involves identifying the specific rock structure and landslide sliding conditions at the research site. Lithology and landslide sliding conditions obtained from the research results serve as crucial references in determining suitable mitigation strategies for landslide disasters. Modeling based on the measurement results of 2D and 3D Electrical Resistivity Tomography (ERT) Geoelectric methods helps provide information on rock layers prone to landslide sliding, with a high sensitivity to rock material up to a depth of 100 meters.. This study aims to measure and assess the sliding plane on the mountain road utilizing 2D Geoelectric and 3D ERT measurements.

## GEOLOGICAL SETTING

Barisan Mountains dominate the Bengkulu quadrangle, with the eastern part belonging to the South Sumatra Basin and the western part to the Bengkulu Basin. The study area is a plateau situated on the Sumatra fault zone, associated both faults, namely the Ketaun faults and Musi-Keruh faults, alluvium and volcanic product (Figure 1). The elevation on this plateau reaches up to 500 meters above sea level. The oldest exposed unit is the Seblat Formation, comprising limestone, and sedimentary clastic derived from volcanic product of the Barisan Mountains. The Simpangaur Formation consists of shallow marine sediment including lignite coal and muddy freshwater deposits. Taxonomically overlying the Simpangaur Formation is the Plio-

Pleistocene-aged Bintunan Formation. This formation forms part of the Barisan volcanic chain, stretching along the western part and paralleling the long axis of Sumatra Island. It served as an area of magmatic activity since the tertiary periods. Starting from the upper part of the Middle Miocene onwards, the volcanic rock composition of the Barisan Line becomes more diverse, ranging from andesite-basalt to dacite-rhyolite, indicating the maturity level of the volcanic arc. The elusive volcanic rock units include QTv and other formations.

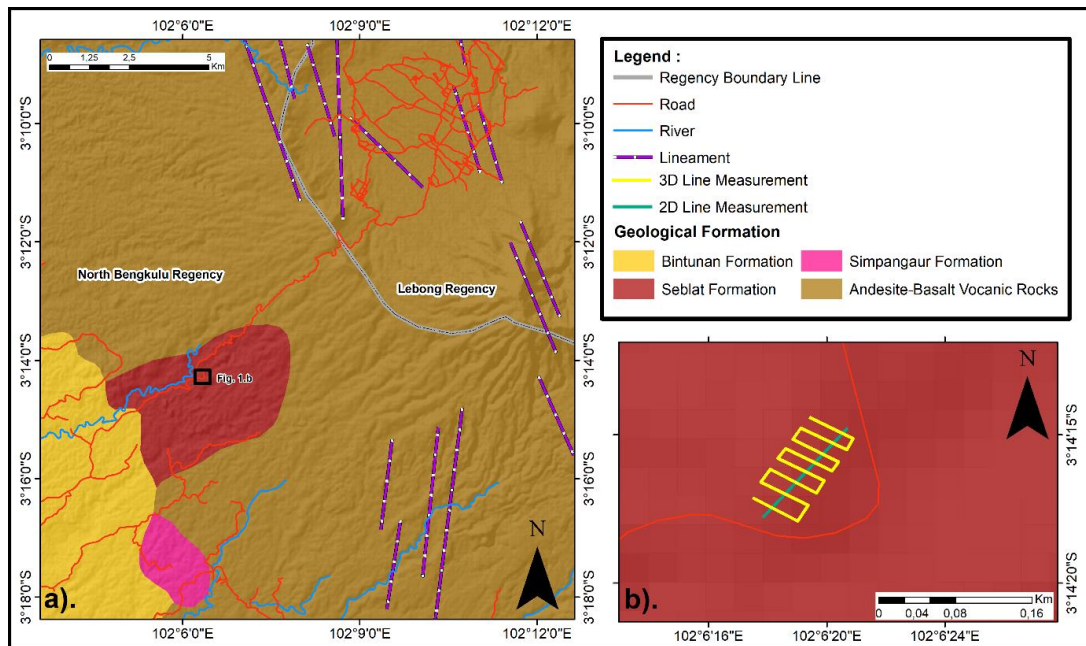
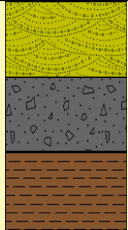
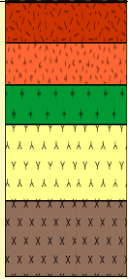


Figure 1. (a) Local geological formation, adapted from Gafoer et al. (2007); (b). 3D and 2D Geoelectric survey line

Table 1. Units of geology at research sites, modified from Gafoer et al., (2012).

Unit	Age	Code	Thickness	Lithology	Notes
Seblat Formation	Late Oligocene – Middle Miocene	Toms	Minimum 750 m		<p><b>Sandstone:</b> Brownish-grey color, medium to coarse, parallel lamination, and grained bedding.</p> <p><b>Conglomerate:</b> Compact with clasts of afford rock.</p> <p><b>Limestone:</b> Yellowish-white in color and contain foraminifera, as do the marls.</p> <p><b>Claystone:</b> Partly calcareous, thinly bedded.</p>
Simpangaur Formation	Late Miocene – Early Pliocene	Tmps	Minimum 500 m		<p><b>Conglomerate:</b> Yellowish-brown to gray in color, medium sorted with clasts 0.3-1.0 cm of andesite, tuff, and altered rock.</p> <p><b>Breccia:</b> Medium-sorted fragments of andesite, tuff dacite, and basalt.</p> <p><b>Sandstone:</b> Medium grained and carbonaceous.</p> <p><b>Claystone:</b> Both carbonaceous &amp; calcareous beds 10-40 cm thick, freshwater Mollusca.</p>

Bintunan Formation	Plio - Pleistocene	QTb	About 200 m	 <p><b>Conglomerate:</b> Yellow-grey color, medium sorted, comprises clasts of andesite, pumice, tuff, slate, and altered rock.</p> <p><b>Breccia:</b> Black-grey color, dominated by volcanic fragments, especially lava.</p> <p><b>Claystone:</b> Brownish-grey, soft and friable, tuffaceous with pumice and silicified wood, also lignite intercalations.</p>
Rhyno-andesite Volcanics	Plio - Pleistocene	QTV	About 350 m	 <p><b>Lavas:</b> Rhyolite, dacite, and andesite lavas are mainly aphanitic but, sometimes, prophyritic the andesite. Locally "sheet lavas" occur, for example, in Pikai and Air Rupit.</p> <p><b>Hybrid Tuff:</b> Yellowish-white in color, carbonaceous with pumice and silicified wood.</p> <p><b>Lithic Tuffs:</b> Khaki to brown-grey in color, generally poorly sorted, 0.3-1.0 cm, angular to subrounded clasts, and up to 30% Volcanic glass.</p>

**METHODS**

The study was conducted in a mountainous area along the North Bengkulu-Lebong mountain road in Bengkulu Province. Geo-electrical measurements were carried out using 2D and 3D Electrical Resistivity Tomography (ERT) for data acquisition. The study involved one 2D measurement point and one 3D ERT measurement point. 3D measurements produce resistivity changes in the X, Y, Z, and 2D X, Y directions (Figure 2) (Eze et al., 2022). Observations method can estimate the actual resistivity value in each rock layer (Bou-Hamdan & Abbas, 2022). The measurement track length was 480 meters with 48 electrodes, spaced 10 meters apart, and oriented in the north direction. Measurements utilized the Wenner-Schlumberger configuration. The data acquisition technique involves injecting an electric current into the subsurface and obtaining the electric potential value from the rock response beneath the ground surface (Reynolds, 1997). The governing equations for 2D and 3D modeling are provided by Zhou & Greenhalgh (2001):

$$2D \text{ Modeling: } \nabla \cdot (\sigma \nabla \hat{G}) + K^2 y \hat{G} = \frac{-\sigma(x-x_s)}{2} \tag{1}$$

$$3D \text{ Modeling: } \nabla \cdot (\sigma \nabla G) = -I \delta(x - x_s) \tag{2}$$

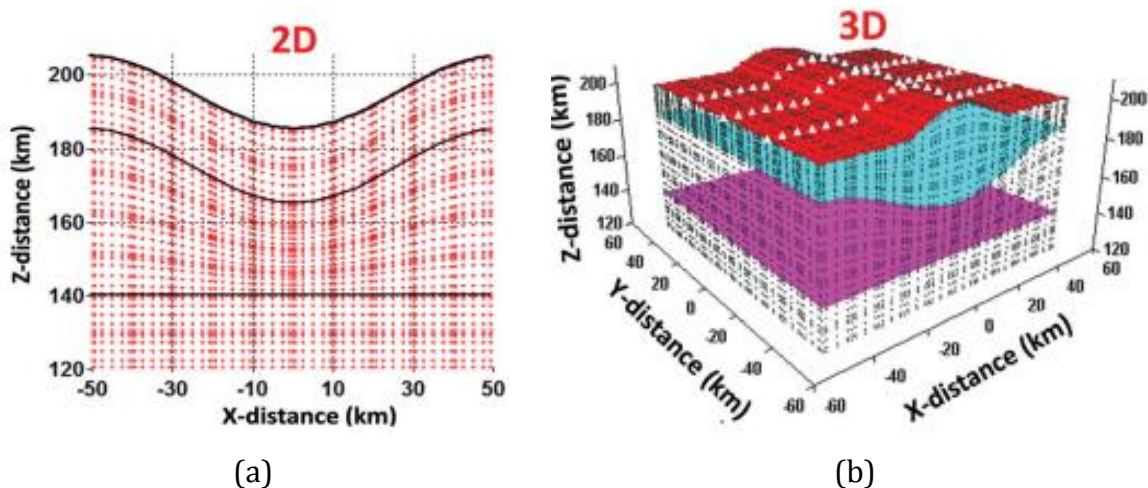


Figure 2. Illustration (a). 2D model, and (b) 3D model (Zhou, 2018).

The 2D data were processed using Excel and Res2Dinv software to generate a 2D cross-sectional model accounting for topographic effects. The 3D model was obtained using ERTLab and ViewLab software. The analysis of both 2D and 3D models takes into consideration the geological conditions, slope, and topography of the study site.

## RESULTS AND DISCUSSION

Because of its highly complex deformation features, rotational landslides constitute a distinct category. Typically, rotational landslides involve arc-shaped, deeply buried, and large-scale sliding surfaces (Ma et al., 2023). Rotational landslides undergo a complex process characterized by strong and recurrent slope instability (Frattini et al., 2018). These rotating landslides can pose a threat to infrastructure and individuals. Consequently, it is crucial to understand the features and processes associated with rotational landslides (Ma et al., 2023).

The mountain road is in a condition that makes the constituent materials on this slope prone to landslides, causing them to easily cascade and overlap surrounding objects. The volume of material involved in landslides increases with the slope angle (Chen et al., 2016). The hill at the research site (Figure 3) has a slope angle ranging from 35° to 55° and decreases by 4° to 8° at the ground surface, where the North Bengkulu-Lebong Mountain road is located. The slope angle of 35°-55° is notably steep and poses a high potential for landslides.

ERT is an in-situ geophysical technique that integrates resistivity profile surveys with vertical electrical prospecting. The ERT approach accurately depicts the electrical resistivity distribution in the subsurface in high-resolution 2D or 3D, based on the fluctuation in resistivity values between the landslide material and the bedrock (Bichler et al., 2004). One of the applications of the ERT approach is the examination of landslides. The planar geometry of landslides and the subsurface aquifers with significant water content can be identified using 2D and 3D ERT approaches (Perrone et al., 2014; Bellanova et al., 2018). When observing landslides, the ERT approach stands out as one of the most effective resources for examining the causes of mass movements linked to water infiltration and temporal and geographical variations in soil moisture. In time series approach, resistivity images are substantially related to time, particularly changes in soil water content and subsoil (Lapenna & Perrone, 2022).

The 2D field data were processed using Res2Dinv software, and the 3D field data were processed using ERTLab 64 software. The model obtained from the data processing process reveals deviations from the field values to the earth resistivity values. The difference between the obtained and actual resistivity values is referred to as the Root Mean Square Error (RMSE), which can be minimized by iteratively repeating the data. Thus, to reduce the RMSE value, a least squares optimization method is applied in the subsequent stages of data acquisition (Lesparre et al., 2016).

The 2D model (Figure 4) depicts the complex stratigraphy of the study site. This research specifically examines the layer prone to landslide sliding. The 2D stratigraphic model generated from measurements at the research site is presented in Figure 4, along with the interpretation results for each rock layer shown in Table 2. The continuous wet clay rock layer from 0-480 meters is a potential subsidence-prone layer. The aquifer layer present at this location is one of the contributing factors to the overlying rock layer's susceptibility to land movement, serving as an initial cause for potential landslides. Factors contributing to landslides in this area are influenced by the rock structure, which is dominated by soft rock, an extreme slope, slope failure in the clay layer (evenly distributed), and hydrology in the study area. The results of the 2D model reveal the presence of rock intrusion and weathered intrusive rocks. This rock intrusion leads to uneven aquifer distribution and undulation in the study area.

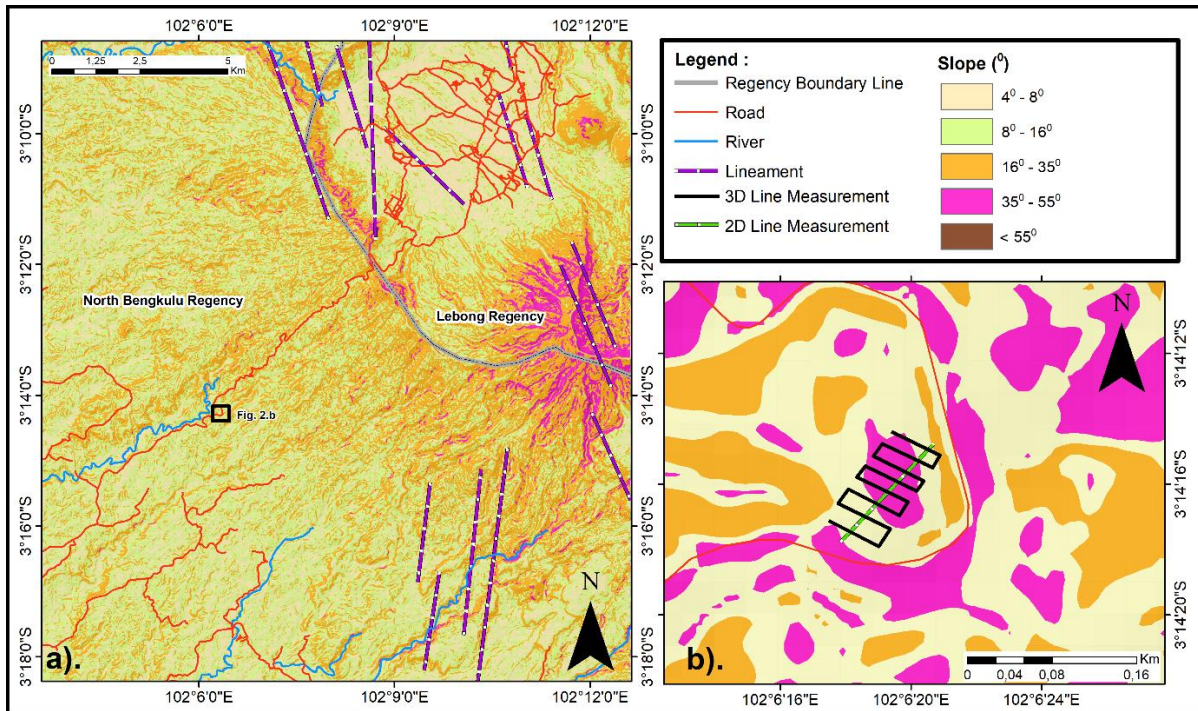


Figure 3. (a). Local map of the slope; (b). Overlay of a 3D and 2D geoelectric survey line with slope map.

The 3D model (Figure 4) shows the continuity of each rock layer to a depth of 80 meters in the X, Y, and Z directions on the North Bengkulu-Lebong mountain road. In the 3D measurements, resistivity values are scattered, with low resistivity values (115-500  $\Omega\text{m}$ ) believed to indicate water-saturated layers, and some spots with high resistivity values (1000-10000  $\Omega\text{m}$ ), considered to be high porosity layers. The layer with a high resistivity value in the topsoil corresponds to a layer of soil resulting from the weathering of plants, often referred to as humus soil, while the high resistivity value (>10000) below 60 meters is fresh massive rock. Resistivity values generally decrease with porosity because the electrical properties in the subsurface are influenced by the quantity and quality of groundwater trapped in rock pores (Paraskevoulakos et al., 2023).

Table 2. Interpretation of each layer on 2D modeling

Layer	Resistivity ( $\Omega\text{m}$ )
Clay	200-500 $\Omega\text{m}$
Aquifer	10-65 $\Omega\text{m}$
Perched Aquifer	100-200 $\Omega\text{m}$
Weathering Clay	500-1000 $\Omega\text{m}$
Wet Clay	500-900 $\Omega\text{m}$
Dry Clay	1000-3000 $\Omega\text{m}$
Weathering Igneous Rock	>10000 $\Omega\text{m}$
Massive Intrusive Rock	>20000 $\Omega\text{m}$

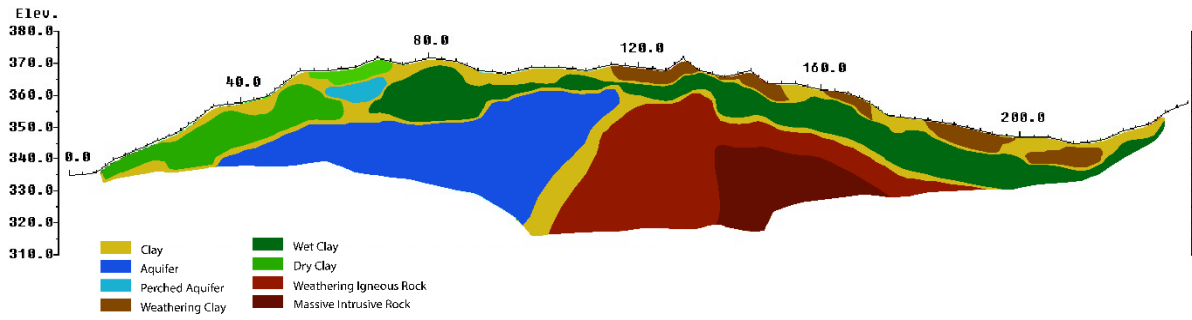


Figure 4. 2D modeling of research sites

ERT measurements can be integrated or compared to data from meteorological, hydrological, and other geophysical techniques (Zieher et al., 2017; Hojat et al., 2019). By comparing and integrating different methods and techniques, the limitations and shortcomings of each method can be addressed, leading to optimal results. Furthermore, the integrated results suggest that ERT efficiency can provide quantitative information on water content and indicate preferred pathways for groundwater intrusion. The capabilities of the ERT method make it highly valuable for better assessment and study of the effects of water saturation to estimate precipitation thresholds in early warning systems for landslides (Lapenna & Perrone, 2022).

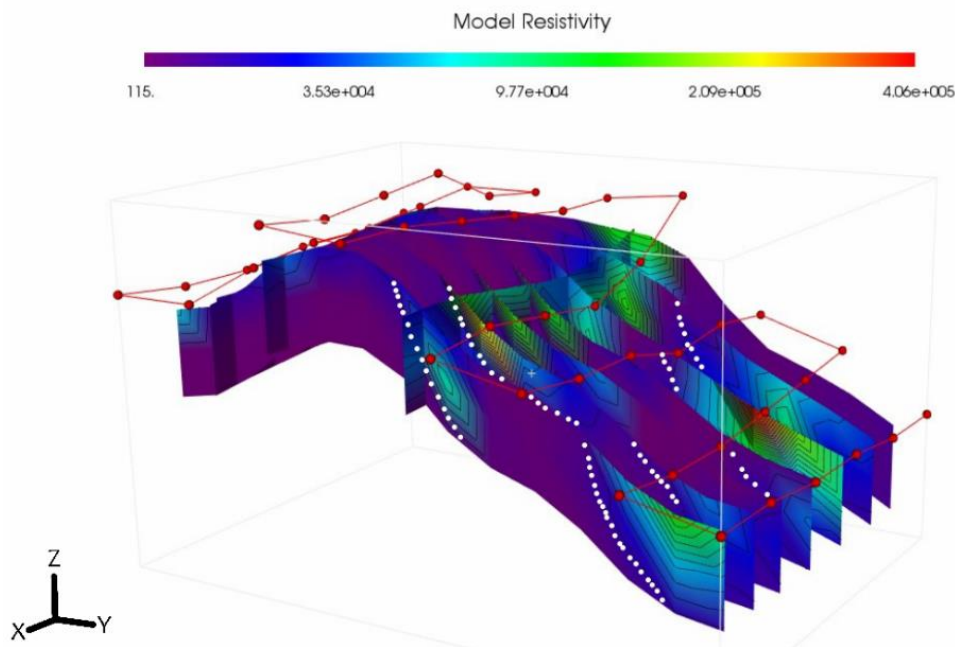


Figure 5. 3D modeling of research sites

The results of the 3D modeling reveal the presence of two landslide slidings at a single landslide location (Figure 5), contributing to a larger volume of landslide material. This occurrence is suspected to be caused by subsurface water. The groundwater layer is unevenly distributed and is constrained by an impermeable clay layer. The undulating topography of the study area leads to uneven distribution and accumulation of the groundwater layer in the slope basin. This

phenomenon is influenced by the downward infiltration of water due to the force of gravity. The schematic representation of this process can be observed in [Figure 6](#).



Figure 6. Illustration of landslide sliding in the study area, which has two landslides sliding in one landslide location ([Frattini et al., 2018](#))

The water layer significantly influences the condition, shape, and distribution of the landslide sliding on a particular slope. The slope of the landslide sliding at the research location does not exhibit uniform conditions ([Figure 6](#)). This variability is a factor that renders an area susceptible to landslides. The presence of the slip plane at this location means that not the entire North Bengkulu-Lebong Mountain road is prone to landslide disasters. The case study in this research affirms that each landslide location has a unique condition for the slip plane, even when situated in the same area. This variability makes the case study of landslides particularly intriguing for research.

The displacement of landslides occurring along the main landslide area can reveal different kinematic behaviors of rotational landslides ([Frattini et al., 2018](#)). Moreover, changes in the sliding surface may lead to exceedingly complex patterns of landslide material displacement. Consequently, we investigated the kinematic behavior of rotating landslides using 2D and 3D ERT observations. Fieldwork was employed to distinguish distinct types of landslides and to determine depth, secondary landslide reach, and secondary embankment sites, in addition to defining the geometry of the sliding surface ([Ma et al., 2023](#)).

## CONCLUSION

The landslide that closed the North Bengkulu-Lebong Mountain Road had a devastating impact on road users and economic activity. The landslide was caused by two sliding events on the cliff section of the road. The layers prone to landslide movements at the research location are composed of clay and wet clay rocks. The impermeable nature of this clay layer makes it susceptible to soil movement. The primary factor at the landslide location on the North Bengkulu-Lebong Mountain Road is the extreme slope, making the clay layer prone to displacement and resulting in the material above it undergoing landslides. This situation leads to continuous landslides on the Bengkulu Utara-Lebong Mountain Road. The findings of this research can serve as a basis for further studies on mitigation strategies, such as selecting appropriate materials for building retaining walls and designing reconstruction models. Implementing such measures can contribute to resolving landslide issues on the Bengkulu Utara-Lebong Mountain Road.

## ACKNOWLEDGMENTS

Authors would like to thank the Research Institutions and Community Service (LPPM), the University of Bengkulu, for the Research Fundamental 2007/UN30.15/PP/2022 grant to support this work financially. The authors also thank the Physics Laboratory, University of Bengkulu, for providing equipment and software during this work.

## DECLARATIONS

### Conflict of Interest

We declare no conflict of interest, financial or otherwise.

### Ethical Approval

On behalf of all authors, the corresponding author states that the paper satisfies Ethical Standards conditions, no human participants, or animals are involved in the research.

### Informed Consent

On behalf of all authors, the corresponding author states that no human participants are involved in the research and, therefore, informed consent is not required by them.

## DATA AVAILABILITY

Data used to support the findings of this study are available from the corresponding author upon request.

## REFERENCES

- Agliardi, F., Crosta, G. B., & Frattini, P. (2013). Slow rock-slope deformation. *Landslides*, 207–221. <https://doi.org/10.1017/cbo9780511740367.019>
- Ariyanto, S. V., & Joni, I. (2019). Zone landslide analysis using geophysical method and analysis of soil type for disaster mitigation in Waru Pamekasan. *Indonesian Journal of Applied Physics*, 9(02), 68. <https://doi.org/10.13057/ijap.v9i2.34520>
- Bell, R., Glade, T., Kruse, J. E., Garcia, A., & Hordt, A. (2006). Etudes de subsurface des glissements de terrain á l' aide de mè thodes gè ophysiques. Applications gè oè lectriques dans l' Alb souabe (Allemagne). *Geographica Helvetica*, 61(3), 201–209. <https://doi.org/10.5194/gh-61-201-2006>
- Bellanova, J., Calamita, G., Giocoli, A., Luongo, R., Macchiato, M., Perrone, A., Uhlemann, S., & Piscitelli, S. (2018). Electrical Resistivity Imaging for the Characterization of the Montaguto Landslide (Southern Italy). *Engineering Geology*, 243, 272–281. <https://doi.org/https://doi.org/10.1016/j.enggeo.2018.07.014>
- Bichler, A., Bobrowsky, P., Best, M., Douma, M., Hunter, J., Calvert, T., & Burns, R. (2004). Three-dimensional mapping of a landslide using a multi-geophysical approach: the quesnel forks landslide. *Landslides*, 1, 29–40. <https://doi.org/10.1007/s10346-003-0008-7>
- BMKG. (2012). *Annual Report of Bengkulu Province*. Badan Meteorologi, Klimatologi, dan Geofisika Provinsi Bengkulu.
- Bou-Hamdan, K. F., & Abbas, A. H. (2022). Utilizing ultrasonic waves in the investigation of contact stresses, areas, and embedment of spheres in manufactured materials replicating proppants and brittle rocks. *Arabian Journal for Science and Engineering*, 47(9), 11635–11650. <https://doi.org/10.1007/s13369-021-06409-6>

- Boyd, J., Chambers, J., Wilkinson, P., Peppas, M., Watlet, A., Kirkham, M., Jones, L., Swift, R., Meldrum, P., Uhlemann, S., & Binley, A. (2021). *A linked geomorphological and geophysical modelling methodology applied to an active landslide*. Springer, 18(8), 2689–2704. <https://doi.org/10.1007/s10346-021-01666-w>
- BPBD. (2019). *Disaster Report of Bengkulu Province 2019*. Badan Penanggulangan Bencana Daerah Provinsi Bengkulu.
- Chen, X. L., Liu, C. G., Chang, Z. F., & Zhou, Q. (2016). The relationship between the slope angle and the landslide size derived from limit equilibrium simulations. *Geomorphology*, 253, 547–550. <https://doi.org/10.1016/j.geomorph.2015.01.036>
- Dai, F. C., Lee, C. F., & Ngai, Y. Y. (2002). Landslide risk assessment and management: An overview. *Engineering Geology*, 64(1), 65–87. [https://doi.org/10.1016/S0013-7952\(01\)00093-X](https://doi.org/10.1016/S0013-7952(01)00093-X)
- Eze, S. U., Abolarin, M. O., Ozegin, K. O., Bello, M. A., & William, S. J. (2022). Numerical modeling of 2-D and 3-D geoelectrical resistivity data for engineering site investigation and groundwater flow direction study in a sedimentary terrain. *Modeling Earth Systems and Environment*, 8(3), 3737–3755. <https://doi.org/10.1007/s40808-021-01325-y>
- Frattini, P., Crosta, G. B., Rossini, M., & Allievi, J. (2018). Activity and kinematic behaviour of deep-seated landslides from PS-InSAR displacement rate measurements. *Landslides*, 15, 1053–1070. <https://doi.org/10.1007/s10346-017-0940-6>
- Gafoer, S., Amin, T., & Pardede, R. (2012). *Geological map of the Bengkulu quadrangle, Sumatera*. Pusat Penelitian dan Pengembangan Geologi.
- Gafoer, S., Amin, T., & Pardede, R. (2007). *Geological map of the Bengkulu quadrangle, Sumatera*. Pusat Penelitian dan Pengembangan Geologi.
- Grifka, J., Weigand, M., Kemna, A., & Heinze, T. (2022). Impact of an uncertain structural constraint on electrical resistivity tomography for water content estimation in landslides. *Land*, 11(8). <https://doi.org/10.3390/land11081207>
- Hojat, A., Arosio, D., Ivanov, V. I., Longoni, L., Papini, M., Scaioni, M., Tresoldi, G., & Zanzi, L. (2019). Geoelectrical characterization and monitoring of slopes on a rainfall-triggered landslide simulator. *Journal of Applied Geophysics*, 170, 103844. <https://doi.org/10.1016/j.jappgeo.2019.103844>
- Huang, R., & Fan, X. (2013). The Landslide Story. *Nature Geoscience*, 6(5), 325–326. <https://doi.org/10.1038/ngeo1806>
- Hugenschmidt, J. (2010). *Geophysics and non-destructive testing for transport infrastructure, with special emphasis on ground penetrating radar*. Doctoral dissertation, ETH Zurich.
- Ismail, M. A., Samsudin, A. R., Mohd Nayan, K. A., & Rafek, A. G. (2002). Penggunaan Teknik Gelombang Permukaan (SASW) dalam Kajian Geologi Kejuruteraan. *Bulletin of the Geological Society of Malaysia*, 45(1), 329–334. <https://doi.org/10.7186/bgsm45200251>
- Jongmans, D., & Garambois, S. (2007). Geophysical investigation of landslides : a review. *Bulletin Société Géologique de France*, 178 (2), 101–112.

- Lapenna, V., Lorenzo, P., Perrone, A., Piscitelli, S., Sdao, F., & Rizzo, E. (2003). High-resolution geoelectrical tomographies in the study of Giarrossa landslide (southern Italy). *Bulletin of Engineering Geology and the Environment*, 62(3), 259–268. <https://doi.org/10.1007/s10064-002-0184-z>
- Lapenna, V., & Perrone, A. (2022). Time-Lapse Electrical Resistivity Tomography ( TL-ERT ) for Landslide Monitoring: Recent Advances and Future Directions. *Applied Sciences (Switzerland)*, 12, 1425. <https://doi.org/https://doi.org/10.3390/app12031425>
- Lesparre, N., Boyle, A., Grychtol, B., Cabrera, J., Marteau, J., & Adler, A. (2016). Electrical resistivity imaging in transmission between surface and underground tunnel for fault characterization. *Journal of Applied Geophysics*, 128, 163–178. <https://doi.org/10.1016/j.jappgeo.2016.03.004>
- Ma, S., Qiu, H., Zhu, Y., Yang, D., Tang, B., Wang, D., Wang, L., & Cao, M. (2023). Topographic Changes, Surface Deformation and Movement Process before, during and after a Rotational Landslide. *Remote Sensing*, 15, 662. <https://doi.org/10.3390/rs15030662>
- Maslin, A. (2015). *Monitoring Ground Vibration arising from Piling and Civil Engineering Projects*. Accudata, 1–7.
- Ouimet, W. B., Whipple, K. X., Royden, L. H., Sun, Z., & Chen, Z. (2007). The influence of large landslides on river incision in a transient landscape: Eastern margin of the Tibetan Plateau (Sichuan, China). *Bulletin of the Geological Society of America*, 119(11–12), 1462–1476. <https://doi.org/10.1130/B26136.1>
- Paraskevoulakos, C., Roebuck, B., Hallam, K. R., & Flewitt, P. E. J. (2023). Temperature dependence of electrical resistivity, deformation, and fracture of polygranular graphite with different amounts of porosity. *SN Applied Sciences*, 5, 28. <https://doi.org/10.1007/s42452-022-05243-1>
- Perrone, A., Lapenna, V., & Piscitelli, S. (2014). Electrical resistivity tomography technique for landslide investigation: a review. *Earth-Science Reviews*, 135, 65–82. <https://doi.org/10.1016/j.earscirev.2014.04.002>
- Reynolds, J. M. (1997). *An Introduction to Applied and Environmental Geophysics*. John Wiley & Sons Ltd, Baffins Lane, Chichester, West Sussex PO19 1UD.
- Shevnin, V., Mousatov, A., Ryjov, A., & Delgado-rodriquez, O. (2007). Estimation of clay content in soil based on resistivity modelling and laboratory measurements. *Geophysical Prospecting*, 55(2), 265–275. <https://doi.org/10.1111/j.1365-2478.2007.00599.x>
- Smethurst, J. A., Smith, A., Uhlemann, S., Wooff, C., Chambers, J., Hughes, P., Lenart, S., Saroglou, H., Springman, S. M., Löfroth, H., & Hughes, D. (2017). Current and future role of instrumentation and monitoring in the performance of transport infrastructure slopes. *Quarterly Journal of Engineering Geology and Hydrogeology*, 50(3), 271–286. <https://doi.org/10.1144/qjegh2016-080>
- Soeters, R., & Van Westen, C. J. (1996). Slope instability recognition, analysis and zonation. *Landslides: investigation and mitigation*, 247, 129–177.
- Souisa, M., Hendrajaya, L., & Handayani, G. (2018). Analisis bidang longsor menggunakan pendekatan terpadu geolistrik, geoteknik dan geokomputer di Negeri Lima Ambon. *Indonesian Journal of Applied Physics*, 8(1), 13. <https://doi.org/10.13057/ijap.v8i1.15482>

- Sugito, I. Z., & Jati, I. P. (2010). Investigasi bidang gelincir tanah longsor menggunakan metode geolistrik tahanan jenis di Desa Kebarongan Kec. Kemranjen Kab. Banyumas. *Berkala Fisika*, 13(2), 49–54.
- Supper, R., Ottowitz, D., Jochum, B., Kim, J. H., Römer, A., Baron, I., Pfeiler, S., Lovisolo, M., Gruber, S., & Vecchiotti, F. (2014). Geoelectrical monitoring: An innovative method to supplement landslide surveillance and early warning. *Near Surface Geophysics*, 12(1), 133–150. <https://doi.org/10.3997/1873-0604.2013060>
- Wieczorek, G. F., & Jäger, S. (1996). Triggering mechanisms and depositional rates of postglacial slope-movement processes in the Yosemite Valley, California. *Geomorphology*, 15(1), 17–31. [https://doi.org/10.1016/0169-555X\(95\)00112-I](https://doi.org/10.1016/0169-555X(95)00112-I)
- Zhou, B. (2018). *Electrical Resistivity Tomography: A Subsurface-Imaging Technique*. *Applied Geophysics with Case Studies on Environmental, Exploration and Engineering Geophysics*. IntechOpen. <https://doi.org/10.5772/intechopen.81511>
- Zhou, B., & Greenhalgh, S. A. (2001). Finite element three-dimensional direct current resistivity modelling: Accuracy and efficiency considerations. *Geophysical Journal International*, 145(3), 679–688. <https://doi.org/10.1046/j.0956-540X.2001.01412.x>
- Zieher, T., Markart, G., Ottowitz, D., Römer, A., Rutzinger, M., Meißl, G., & Geitner, C. (2017). Water content dynamics at plot scale – comparison of time-lapse electrical resistivity tomography monitoring and pore pressure modelling. *Journal of Hydrology*, 544, 195–209. <https://doi.org/10.1016/j.jhydrol.2016.11.019>